JOURNAL OF COMPUTATIONAL PHYSICS **147,** 1–21 (1998)
ARTICLE NO. CP986021

Spectral Analysis of Symmetric Operators: Application to the Laplace Tidal Model

A. I. Yaremchuk* and J. Schröter†,[1]

**Andreyev Acoustics Institute, Shvernika 4, 117034 Moscow, Russia;*
†*Alfred-Wegener Institute, Bremerhaven, Germany*
E-mail: jgs@awi-bremerhaven.de

Received October 21, 1997; revised March 27, 1998

A finite-storage iterative algorithm is proposed for performing spectral analysis and synthesis with respect to an arbitrary symmetric operator. This operator can be of any nature, and it is only necessary to define its action. The whole analysis may be performed by a repeated application of the operator. Compared with traditional methods, our approach allows us to treat discrete systems of very high dimension. As an example, we consider in the framework of an ocean governed by the Laplace tidal equations the problem of separation of large-scale geostrophic modes and surface-waves contributing to a given flow. As a second example we apply the algorithm to a problem in satellite remote sensing. We reconstruct the mean large-scale oceanic circulation from observed sea surface height data. In the case of a synthetic data set the agreement of analytical and numerical results is satisfactory.

Key Words: spectrum; eigenvalues; singular values; inverse problems.

1. INTRODUCTION

Frequently the analysis of physical phenomena rests on the ability to investigate into spectral properties of differential operators and to relate experimental data to them. Examples include determination of resonant frequencies, density of states, shapes of exited vibrational modes, distribution of energy over the spectrum, etc. The related operators in Hilbert spaces typically are self-adjoint and their structure may be interpreted in terms of eigenvalues and eigenvectors, even if they possess continuous spectra.

In conventional numerical analysis the original operator is approximated by a finite-rank model which provides estimates for distribution of eigenvalues and related amplitudes of decomposition of data into a sum of eigenvectors. However, although the spectrum of a finite-rank model is always discrete, at certain scales its density may be so high (this will

[1] Corresponding author.

0021-9991/98 $25.00

certainly be the case when we try to approximate continuous spectra) that it may look like a continuous one. Numerically it might be impossible to evaluate the eigenvalues and eigenvectors explicitly. Fortunately, in such cases only projectors on finite spectral bands or, equivalently, only sums of eigenvectors over wide ranges of indices are of physical interest.

In the following we propose a method for evaluating arbitrary functions of finite-rank self-adjoint operators, which allows an effective solution for any problem of spectral analysis/synthesis connected with a numerical model of an operator under consideration. The described method accesses the operator only via its action. Thus, the user only needs to provide a subroutine which computes the product of the operator and a vector. Only a small number of vectors resulting from successive iterations must be stored in memory; this makes it possible to study very high-dimensional problems which otherwise could not be treatable.

We shall show how a function of an operator can be represented by a polynomial expansion. Especially inverse problems are considered by studying the singular value decomposition. After reviewing basic properties of symmetric operators in Section 2, we develop in Section 3 a computational approach for evaluating functions of real symmetric and antisymmetric operators. In Section 4 we demonstrate how the method can be applied to performing a singular value decomposition, and in Section 5 we present an illustrative example of spectral analysis of the Laplace tidal model and separate surface waves and geostrophic motions in its framework. Section 6 is devoted to an application of our method to the solution of inverse problems in the spirit of singular value decomposition. By considering the problem of reconstructing oceanic circulation from observed sea surface elevation data we demonstrate performance of the method in spectral synthesis. The final section contains concluding remarks.

2. OPERATOR-VALUED FUNCTIONS

Let us first describe our notation. Throughout the article we shall consider vector spaces over the field of real numbers supplied with a Euclidean structure and use Dirac's bra–ket notation to distinguish between column and row vectors.

In order to specify a Euclidean structure, we need a symmetric positive Gram's matrix, g, which determines the scalar product $(\psi, \psi') \stackrel{\text{def}}{=} \langle\psi|g|\psi'\rangle$.

Given a linear operator $\mathcal{H}$, we define its adjoint, $\mathcal{H}^\dagger$, by means of the equation $(\mathcal{H}^\dagger\psi, \phi) = (\psi, \mathcal{H}\phi)$. In matrix notation $\mathcal{H}^\dagger = g^{-1}\mathcal{H}^{\mathrm{T}}g$, where $\mathcal{H}^{\mathrm{T}}$ means transpose. An operator is called symmetric (self-adjoint) if it coincides with its adjoint. Similarly, an operator $\mathcal{L}$ is antisymmetric, if it is opposite to its adjoint, i.e., if $\mathcal{L}^\dagger = -\mathcal{L}$. In the following treatment we shall always assume that $\mathcal{H}$ is a symmetric operator, and $\mathcal{L}$ is antisymmetric.

The spectral theorem claims that for any symmetric operator $\mathcal{H}$ acting in a D-dimensional Euclidean space there exists a complete orthonormal set $|\psi_1\rangle, \ldots, |\psi_D\rangle$ of its eigenvectors and a corresponding set $\varepsilon_1, \ldots, \varepsilon_D$ of eigenvalues:

$$\langle\psi_i|g|\psi_k\rangle = \delta_{ik}, \quad i, k = 1, \ldots, D, \tag{1}$$

$$\mathcal{H}|\psi_k\rangle = \varepsilon_k|\psi_k\rangle. \tag{2}$$

Operators defined by $\mathcal{P}_k \stackrel{\text{def}}{=} |\psi_k\rangle\langle\psi_k|g$ are also self-adjoint and are called spectral projectors, since $\mathcal{P}_k^2 = \mathcal{P}_k$. They supply us with a partition of unity:

$$1 = \sum_k \mathcal{P}_k. \tag{3}$$

The symmetric bilinear form g, defining the scalar product, and operator $\mathcal{H}$ also may be decomposed:

$$g = \sum_k g|\psi_k\rangle\langle\psi_k|g, \tag{4}$$

$$\mathcal{H} = \sum_k \varepsilon_k \mathcal{P}_k = \sum_k \varepsilon_k |\psi_k\rangle\langle\psi_k|g. \tag{5}$$

An anti-symmetric operator $\mathcal{L}$ is characterized with similar properties: there exists a basis $\psi_1, \ldots, \psi_D$ such that (1), (3), (4) are valid, and

$$\mathcal{L} = \sum_k \varepsilon_k |\psi_k\rangle\big\langle\psi_{\sigma(k)}\big|g,$$

$$\mathcal{L}|\psi_k\rangle = \varepsilon_k \big|\psi_{\sigma(k)}\big\rangle,$$

with

$$\varepsilon_{\sigma(k)} = -\varepsilon_k. \tag{6}$$

Here σ is an involution acting in the space of indices: $\sigma(\sigma(k)) = k$. The spectrum of an anti-symmetric operator is purely imaginary and coincides with the set $i\varepsilon_1, \ldots, i\varepsilon_D$.

Now we are prepared to define functions of operators. Let $f(\varepsilon)$ be an entire analytic function of a complex parameter ε. This means that f may be represented by a convergent series:

$$f(\varepsilon) = \sum_{n=0}^{\infty} f_n \varepsilon^n.$$

Similarly, we may substitute $\mathcal{H}$ for ε in this formula and obtain

$$f(\mathcal{H}) \stackrel{\text{def}}{=} \sum_{n=0}^{\infty} f_n \mathcal{H}^n \tag{7}$$

$$= \sum_k f(\varepsilon_k)\mathcal{P}_k = \sum_k f(\varepsilon_k)|\psi_k\rangle\langle\psi_k|g. \tag{8}$$

Here the second identity was derived with the aid of $\mathcal{P}_k^n = \mathcal{P}_k$, which holds for any $n > 0$. We see that for evaluation of $f(\mathcal{H})$ only the behavior of $f(\varepsilon)$ at the spectral points ε_k is important. Thus, we can use (8) for computing any function of an operator, provided it is regular on its spectrum. However, formal application of this formula to nonsmooth functions also may make sense. For instance, the function

$$\varepsilon \mapsto \delta(\varepsilon - \mathcal{H}) = \sum_k \delta(\varepsilon - \varepsilon_k)\mathcal{P}_k \tag{9}$$

is connected with the distribution of eigenvalues and eigenamplitudes.

Given any vector $|\mathrm{vac}\rangle$, we may introduce the associated Chellen–Leman spectral function

$$\varrho_{\mathrm{vac}}(\varepsilon) \stackrel{\text{def}}{=} \sum_k \delta(\varepsilon - \varepsilon_k)|\langle\psi_k|g|\mathrm{vac}\rangle|^2 \tag{10}$$

which shows the location of eigenvalues (δ-peaks at $\varepsilon = \varepsilon_k$) and the corresponding amplitudes in the decomposition of $|\mathrm{vac}\rangle$ into a superposition of eigenmodes:

$$|\mathrm{vac}\rangle = \sum_k |\psi_k\rangle\langle\psi_k|g|\mathrm{vac}\rangle.$$

It is easy to see that the Chellen–Leman function is just a certain matrix element of (9):

$$\varrho_{\mathrm{vac}}(\varepsilon) = \langle\mathrm{vac}|g\,\delta(\varepsilon - \mathcal{H})|\mathrm{vac}\rangle.$$

Similarly, the spectral function

$$\varrho_{\mathcal{H}}(\varepsilon) \stackrel{\mathrm{def}}{=} \sum_k \delta(\varepsilon - \varepsilon_k) \tag{11}$$

describes the density of distribution of eigenvalues of $\mathcal{H}$. It may be obtained as a mean of matrix elements over an ensemble of random vectors:

$$\varrho_{\mathcal{H}}(\varepsilon) = \sum_k \delta(\varepsilon - \varepsilon_k)\mathrm{Mean}\left\{|\langle\psi_k|\sqrt{g}|\xi\rangle|^2\right\} \tag{12}$$

$$= \mathrm{Mean}\left\{\langle\xi|\sqrt{g}\delta(\varepsilon - \mathcal{H})\frac{1}{\sqrt{g}}|\xi\rangle\right\}. \tag{13}$$

Here $|\xi\rangle$ is a normally distributed random variable, and $\mathrm{Mean}\{\cdots\}$ denotes the average value. In practice we can only evaluate the mean over a finite ensemble of independent realizations of a stochastic variable $|\xi\rangle$. This implies that our estimate of mean values of squared amplitudes $|\langle\psi_k|\sqrt{g}|\xi\rangle|^2$ on the right-hand side of (12) will be equal to unity only approximately.

For antisymmetric operators we have to use functions which are regular on the imaginary axis in the complex plane. Any function of this type may be uniquely represented as the sum of an even function E and odd function I:

$$f(\varepsilon) = E(-i\varepsilon) + iI(-i\varepsilon). \tag{14}$$

If ε takes real values, the functions $E(\varepsilon)$ and $I(\varepsilon)$ also must be real. The analogue of (8) is

$$f(\mathcal{L}) = E(-i\mathcal{L}) + iI(-i\mathcal{L}), \tag{15}$$

with $\mathcal{L}$ denoting an antisymmetric operator and

$$E(-i\mathcal{L}) = \sum_k E(\varepsilon_k)|\psi_k\rangle\langle\psi_k|g,$$

$$iI(-i\mathcal{L}) = \sum_k I(\varepsilon_k)|\psi_k\rangle\langle\psi_{\sigma(k)}|g.$$

3. EXPANSION IN ORTHOGONAL POLYNOMIALS

In practice in a high-dimensional case it is impossible to evaluate a function of an operator exactly, because we do not know either eigenvalues or eigenvectors beforehand. We only

can evaluate a polynomial function by successively computing $\mathcal{H}, \mathcal{H}^2, \ldots$. (In this section we shall only deal with symmetric operators, since $-i\mathcal{L}$ is self-adjoint and we may use (15) to turn an antisymmetric case into a symmetric one.) Thus, given a function $f(\varepsilon)$, we need to choose a polynomial approximation $P(\varepsilon)$ to it and to evaluate $P(\mathcal{H})$. Since only values $f(\varepsilon_k)$ are important, the approximation must be of high quality only on a finite interval, say $(E_{\min}, E_{\max})$, which contains the spectrum. According to the Weierstrass theorem, a continuous function may be approximated with any accuracy, but practically it is difficult to obtain such an approximation explicitly. A straightforward way is to use the orthogonal polynomial technique. For the sake of brevity here we shall consider only Chebyshev polynomials as suitable for most cases, although sometimes it might be more convenient to use a different basis in the space of all polynomials.

3.1. *Expansion in Chebyshev Polynomials*

Chebyshev polynomials $\mathrm{T}_n(\varepsilon)$ of the first kind (see [1]) form a complete orthogonal set in the space of functions on the interval $(-1, 1)$ with respect to the weight $d\varepsilon/\sqrt{1-\varepsilon^2}$. Since they meet the parity condition

$$\mathrm{T}_n(-\varepsilon) = (-1)^n \mathrm{T}_n(\varepsilon),$$

we can represent an arbitrary even function, $E(\varepsilon)$, and an odd function, $I(\varepsilon)$, as a sum of even and odd polynomials as follows:

$$E(\varepsilon) = \sum_{n=0}^{\infty} a_n \mathrm{T}_{2n}(\varepsilon), \quad I(\varepsilon) = \sum_{n=0}^{\infty} b_n \mathrm{T}_{2n+1}(\varepsilon). \tag{16}$$

Explicit formulas for evaluation of the coefficients a_n and b_n by means of the fast Fourier transform may be found in the appendices. If the spectrum of an operator $\mathcal{H}$ lies in the interval $(-1, 1)$, representations

$$E(\mathcal{H}) = \sum_{n=0}^{\infty} a_n \mathrm{T}_{2n}(\mathcal{H}), \quad I(\mathcal{H}) = \sum_{n=0}^{\infty} b_n \mathrm{T}_{2n+1}(\mathcal{H})$$

are also valid. Introducing

$$|A_n\rangle \stackrel{\text{def}}{=} \mathrm{T}_{2n}(\mathcal{H})|\mathrm{vac}\rangle, \quad |B_n\rangle \stackrel{\text{def}}{=} \mathrm{T}_{2n+1}(\mathcal{H})|\mathrm{vac}\rangle,$$

we obtain

$$E(\mathcal{H})|\mathrm{vac}\rangle = \sum_{n=0}^{\infty} a_n |A_n\rangle, \tag{17}$$

$$I(\mathcal{H})|\mathrm{vac}\rangle = \sum_{n=0}^{\infty} b_n |B_n\rangle. \tag{18}$$

Expansions of this kind may be used for treating any operator. Suppose that the spectrum of $\mathcal{H}$ is contained in the interval $(E_{\min}, E_{\max})$. In order to evaluate $F(\mathcal{H})$, we must compose

an auxiliary operator

$$\mathcal{E} \stackrel{\text{def}}{=} \frac{2}{(E_{\max} - E_{\min})}\left(\mathcal{H} - \frac{E_{\max} + E_{\min}}{2}\right) \tag{19}$$

(its spectrum is contained in the interval $(-1, 1)$), represent an auxiliary function

$$f(\varepsilon) \stackrel{\text{def}}{=} F\left[\frac{E_{\max} + E_{\min}}{2} + \frac{E_{\max} - E_{\min}}{2}\varepsilon\right], \quad |\varepsilon| < 1,$$

in the form

$$f(\varepsilon) = E(\varepsilon) + I(\varepsilon),$$

where $E(\varepsilon)$ is even and $I(\varepsilon)$ is odd, expand them in a series (16), and use

$$F(\mathcal{H}) = f(\mathcal{E}) = \sum_{n=0}^{\infty} \{a_n \mathrm{T}_{2n}(\mathcal{E}) + b_n \mathrm{T}_{2n+1}(\mathcal{E})\}.$$

Similarly,

$$F(\mathcal{H})|\mathrm{vac}\rangle = \sum_{n=0}^{\infty} \{a_n |A_n\rangle + b_n |B_n\rangle\}.$$

The vectors $|A_n\rangle$ and $|B_n\rangle$ can be computed recursively:

$$\begin{aligned} |A_0\rangle &= |\mathrm{vac}\rangle, \quad |B_0\rangle = \mathcal{E}|A_0\rangle, \\ |A_{n+1}\rangle &= 2\mathcal{E}|B_n\rangle - |A_n\rangle, \\ |B_{n+1}\rangle &= 2\mathcal{E}|A_{n+1}\rangle - |B_n\rangle, \quad n \geq 0. \end{aligned}$$

It may be easily shown that

$$|A_n\rangle = \sum_k |\psi_k\rangle (-1)^n \cos(n\theta_k)\langle\psi_k|g|\mathrm{vac}\rangle, \tag{20}$$

$$|B_n\rangle = \sum_k |\psi_k\rangle (-1)^n \sin[(n + 1/2)\theta_k]\langle\psi_k|g|\mathrm{vac}\rangle, \tag{21}$$

$$\varepsilon_k = \frac{E_{\max} + E_{\min}}{2} + \frac{E_{\max} - E_{\min}}{2}\sin(\theta_k/2). \tag{22}$$

3.2. *Digital Filters*

For numerical evaluation we have to truncate the infinite series (16). This procedure may be interpreted in two ways. Either the multiplication of the Fourier coefficients by the factors

$$\kappa_n = \begin{cases} 1, & 0 \leq n \leq N-1, \\ 0, & N \leq n, \end{cases} \tag{23}$$

or the employment of smoothed functions,

$$E(\varepsilon)^{(\text{smoothed})} = \sum_{n=0}^{\infty} \kappa_n a_n \mathrm{T}_{2n}(\varepsilon),$$

$$I(\varepsilon)^{(\text{smoothed})} = \sum_{n=0}^{\infty} \kappa_n b_n \mathrm{T}_{2n+1}(\varepsilon),$$

instead of the actual ones. These smoothed functions (usually referred to as windows) may be obtained as a result of application to $E(\varepsilon)$ and $I(\varepsilon)$ of smoothing Hilbert–Schmidt integral operators of finite rank which are completely determined by the coefficients (23). If only a finite number of coefficients $\{\kappa_n\}$ do not vanish, the smoothed functions appear to be polynomials, as is necessary. However, their behavior depends on the smoothing operators, and we are faced with the problem of choosing the optimum ones. The most simple kernel (23) provides approximation of low quality because of the Gibbs effect. Its improvement is just the problem of digital filter design and is extensively considered in a signal processing (e.g., [2, 3]), so we shall not address it here.

3.3. *Spectral Density and Distribution of Eigenvalues*

Here we shall consider the rescaled operator (19) instead of $\mathcal{H}$ (this surely is not a restriction) and, instead of the spectral function (10), we shall use a more coarse one,

$$\rho_{\text{vac}}(\theta) \stackrel{\text{def}}{=} \sum_k [\delta(\theta - \theta_k) + \delta(\theta + \theta_k)] |\langle \psi_k | g | \text{vac} \rangle|^2,$$

with $\theta_k = 2\arcsin(\varepsilon_k)$. It may be evaluated with the help of the spectral density window determined by a one-parametric family of coefficients

$$a_0 = \frac{1}{\pi}, \quad a_n(\theta) = \frac{2}{\pi}(-1)^n \cos(n\theta), \quad 0 < \theta < \pi. \tag{24}$$

In view of (20)–(22) and the identity

$$\delta(\theta - \theta') + \delta(\theta + \theta') = \sum_{n=0}^{\infty} (-1)^n a_n(\theta) \cos(n\theta') \tag{25}$$

which is valid for $-\pi < \theta, \theta' < \pi$, we conclude that

$$\rho_{\text{vac}}(\theta) = \sum_{n=0}^{\infty} a_n(\theta) \langle \text{vac} | g | A_n \rangle. \tag{26}$$

Note that using this window, we are not able to distinguish contributions coming from the eigenvalues ε_k and $-\varepsilon_k$ to the amplitude of the δ-constituent of $\rho_{\text{vac}}(\theta)$ at $\theta = \theta_k$. In order to distinguish between ε_k and $-\varepsilon_k$, we need to employ an odd spectral density window as well.

Similarly, the distribution of eigenvalues may be described by the function

$$\rho_{\mathcal{H}}(\theta) \stackrel{\text{def}}{=} \sum_k [\delta(\theta-\theta_k)+\delta(\theta+\theta_k)]$$
$$= \sum_{n=0}^{\infty} a_n(\theta)\,\text{Mean}\{\langle \text{vac}|g|A_n\rangle\}, \tag{27}$$

where $|\text{vac}\rangle = g^{-1/2}|\xi\rangle$ and $|\xi\rangle$ stands for a normally distributed random variable.

Truncation $a_n \mapsto \kappa_n a_n$ of any of the above series corresponds to smoothing (convolution) of the corresponding function with the kernel

$$K(\theta) = \frac{1}{\pi}\left\{\frac{\kappa_0}{2} + \sum_{n=1}^{\infty}\kappa_n \cos(n\theta)\right\} \tag{28}$$

on the interval $(-\pi, \pi)$ with periodic boundary conditions.

3.4. *Antisymmetric Operators*

Antisymmetric operators arise as generators of one-parametric groups of orthogonal transformations of an Euclidean space and usually are encountered in evolutionary problems. Here we shall adopt the above formulas to this case in such a manner that only real numbers will appear in the process of computation.

The spectrum of an anti-symmetric real operator, $\mathcal{L}$, is purely imaginary and is invariant with respect to the involution $\varepsilon \mapsto -\varepsilon$, with ε being a complex spectral variable. Introducing a self-adjoint operator $\mathcal{H} \stackrel{\text{def}}{=} -i\mathcal{L}$, $i=\sqrt{-1}$, we can use the previous formulas for processing $\mathcal{H}$. In terms of $\mathcal{L}$ the procedure may be formulated as follows.

In order to evaluate $F(\mathcal{L})$, compose an auxiliary operator $\mathcal{E} = \mathcal{L}/E_{\max}$, where $E_{\max} > 0$ bounds the spectral radius of $\mathcal{L}$ from above, represent a function $\varepsilon \mapsto F(i\varepsilon E_{\max})$ in the form

$$F(i\varepsilon E_{\max}) = E(\varepsilon) + iI(\varepsilon), \quad -1 < \varepsilon < 1,$$

where $E(\varepsilon)$ and $I(\varepsilon)$ are even and odd functions of a real variable ε, and use

$$F(\mathcal{L}) = E(-i\mathcal{E}) + iI(-i\mathcal{E}).$$

Introducing real vectors

$$|A_n\rangle \stackrel{\text{def}}{=} \text{T}_{2n}(-i\mathcal{E})|\text{vac}\rangle, \quad |B_n\rangle \stackrel{\text{def}}{=} i\text{T}_{2n+1}(-i\mathcal{E})|\text{vac}\rangle,$$

we get

$$E(-i\mathcal{E})|\text{vac}\rangle = \sum_{n=0}^{\infty} a_n|A_n\rangle,$$
$$iI(-i\mathcal{E})|\text{vac}\rangle = \sum_{n=0}^{\infty} b_n|B_n\rangle,$$
$$F(\mathcal{L})|\text{vac}\rangle = \sum_{n=0}^{\infty}\{a_n|A_n\rangle + b_n|B_n\rangle\}, \tag{29}$$

as soon as (16) holds. The recursion relation takes the form

$$|A_0\rangle = |\mathrm{vac}\rangle, \quad |B_0\rangle = \mathcal{E}|A_0\rangle,$$
$$|A_{n+1}\rangle = -2\mathcal{E}|B_n\rangle - |A_n\rangle,$$
$$|B_{n+1}\rangle = 2\mathcal{E}|A_{n+1}\rangle - |B_n\rangle, \quad n \geq 0.$$

All other formulas remain unchanged.

4. SINGULAR VALUE DECOMPOSITION

Singular value decomposition (SVD) is a particular application of general spectral theory of self-adjoint operators to the case where a linear operator, $\mathcal{Q}$, maps one Euclidean space into another. It is frequently used in inverse theory and we shall apply it in an example in Section 6. We shall denote vectors from the source space with capital letters and vectors from the target space with small letters. Euclidean structures of the source and target spaces will be specified with the help of the Gram matrices G and g, respectively.

In most applications SVD serves as a tool for solving an over- or under-determined system of equations,

$$\mathcal{Q}|\Phi\rangle = |\mathrm{vac}\rangle,$$

with $|\Phi\rangle$ considered unknown. A straightforward SVD solution is

$$|\Phi\rangle = \sum_{\varepsilon_k} \frac{1}{\varepsilon_k} |\Psi_k\rangle\langle\psi_k|\mathrm{vac}\rangle. \tag{30}$$

Here $\varepsilon_k > 0$ stand for nonzero singular values of $\mathcal{Q}$, $|\Psi_k\rangle$ and $|\psi_k\rangle$ are the corresponding normalized singular vectors in the source and target spaces, respectively.

From a general point of view, singular values arise as the result of spectral decomposition of a self-adjoint operator,

$$\mathcal{H} \stackrel{\mathrm{def}}{=} \begin{bmatrix} 0 & \mathcal{Q} \\ \mathcal{Q}^\dagger & 0 \end{bmatrix}. \tag{31}$$

It is well known that nonzero eigenvalues $E_1, \ldots, E_D$ (D is a certain integer) of operators $\mathcal{Q}^\dagger\mathcal{Q}$ and $\mathcal{Q}\mathcal{Q}^\dagger$ coincide. Let $\{|\Psi_k\rangle\}$ and $\{|\psi_k\rangle\}$ be the corresponding normalized eigenvectors:

$$(\mathcal{Q}^\dagger\mathcal{Q} - E_k)|\Psi_k\rangle = 0, \quad \langle\Psi_k|G|\Psi'_k\rangle = \delta_{kk'}, \tag{32}$$
$$(\mathcal{Q}\mathcal{Q}^\dagger - E_k)|\psi_k\rangle = 0, \quad \langle\psi_k|g|\psi'_k\rangle = \delta_{kk'}. \tag{33}$$

Since all eigenvalues E_k are positive (recall that we are considering only nonzero eigenvalues), we can unambiguously represent them as squares of $\varepsilon_k \stackrel{\mathrm{def}}{=} \sqrt{E_k} > 0$. It can be shown that $\pm\varepsilon_1, \ldots, \pm\varepsilon_D$ appear to be all nonzero eigenvalues of $\mathcal{H}$. Moreover, $|\Psi_k\rangle$ and $|\psi_k\rangle$ can be normalized in such a manner that relations

$$\varepsilon_k|\Psi_k\rangle = \mathcal{Q}^\dagger|\psi_k\rangle, \quad \varepsilon_k|\psi_k\rangle = \mathcal{Q}|\Psi_k\rangle$$

are satisfied.

Let $|\psi_i^{(0)}\rangle$ and $|\Psi_j^{(0)}\rangle$ denote normalized solutions to the equations

$$\mathcal{Q}\big|\psi_i^{(0)}\big\rangle = 0, \quad \mathcal{Q}^\dagger\big|\Psi_j^{(0)}\big\rangle = 0,$$

respectively. It may be shown that vectors $|\psi_k\rangle$ and $|\psi_i^{(0)}\rangle$ form an orthonormal basis in the target space, whereas $|\Psi_k\rangle$ and $|\Psi_j^{(0)}\rangle$ form an orthonormal basis in the source space.

With this notation one can easily verify that given any function $f(\varepsilon)$, the following identity is valid:

$$\begin{aligned} f(\mathcal{H}) = &\sum_k \frac{f(\varepsilon_k)+f(-\varepsilon_k)}{2}\begin{bmatrix} |\psi_k\rangle\langle\psi_k|g & 0 \\ 0 & |\Psi_k\rangle\langle\Psi_k|G \end{bmatrix} \\ &+ \sum_k \frac{f(\varepsilon_k)-f(-\varepsilon_k)}{2}\begin{bmatrix} 0 & |\psi_k\rangle\langle\Psi_k|G \\ |\Psi_k\rangle\langle\psi_k|g & 0 \end{bmatrix} \\ &+ f(0)\sum_i \begin{bmatrix} \big|\psi_i^{(0)}\big\rangle\big\langle\psi_i^{(0)}\big|g & 0 \\ 0 & 0 \end{bmatrix} \\ &+ f(0)\sum_j \begin{bmatrix} 0 & 0 \\ 0 & \big|\Psi_j^{(0)}\big\rangle\big\langle\Psi_j^{(0)}\big|G \end{bmatrix}. \end{aligned} \tag{34}$$

This formula is rather interesting, so let us consider it in detail. In the case of an odd function f, i.e., when $f(-\varepsilon) = -f(\varepsilon)$, (34) takes the form

$$f(\mathcal{H}) = \sum_k f(\varepsilon_k)\begin{bmatrix} 0 & |\psi_k\rangle\langle\Psi_k|G \\ |\Psi_k\rangle\langle\psi_k|g & 0 \end{bmatrix}. \tag{35}$$

Comparing it with (30), we see that the SVD solution (30) is just a component of the vector

$$\begin{bmatrix} 0 \\ |\Phi\rangle \end{bmatrix} = f(\mathcal{H})\begin{bmatrix} |\mathrm{vac}\rangle \\ 0 \end{bmatrix},$$

provided $f(\varepsilon) = 1/\varepsilon$.

In the case of an even function f, where $f(-\varepsilon) = f(\varepsilon)$, (34) takes the form

$$\begin{aligned} f(\mathcal{H}) = &\sum_k f(\varepsilon_k)\begin{bmatrix} |\psi_k\rangle\langle\psi_k|g & 0 \\ 0 & |\Psi_k\rangle\langle\Psi_k|G \end{bmatrix} \\ &+ f(0)\sum_i \begin{bmatrix} \big|\psi_i^{(0)}\big\rangle\big\langle\psi_i^{(0)}\big|g & 0 \\ 0 & 0 \end{bmatrix} \\ &+ f(0)\sum_j \begin{bmatrix} 0 & 0 \\ 0 & \big|\Psi_j^{(0)}\big\rangle\big\langle\Psi_j^{(0)}\big|G \end{bmatrix}. \end{aligned} \tag{36}$$

Since the spectrum of $\mathcal{H}$ is invariant with respect to involution $\varepsilon \mapsto -\varepsilon$, we can use formulas of Section 3.1 for evaluation of

$$F(\mathcal{H})\begin{bmatrix} |\mathrm{vac}\rangle \\ |\mathrm{VAC}\rangle \end{bmatrix}.$$

Assuming that the spectral radius of $\mathcal{H}$ is $E_{\max}$, we may form an auxiliary operator $\mathcal{E} = \mathcal{H}/E_{\max}$, represent an auxiliary function $f(\varepsilon) \stackrel{\text{def}}{=} F(\varepsilon E_{\max})$ as a sum of an even and odd functions $E(\varepsilon)$ and $I(\varepsilon)$, expand them in a series (16), introduce vectors

$$\begin{bmatrix} |u_n\rangle \\ |V_n\rangle \end{bmatrix} \stackrel{\text{def}}{=} \mathrm{T}_{2n}(\mathcal{E}) \begin{bmatrix} |\mathrm{vac}\rangle \\ |\mathrm{VAC}\rangle \end{bmatrix},$$

$$\begin{bmatrix} |v_n\rangle \\ |U_n\rangle \end{bmatrix} \stackrel{\text{def}}{=} \mathrm{T}_{2n+1}(\mathcal{E}) \begin{bmatrix} |\mathrm{vac}\rangle \\ |\mathrm{VAC}\rangle \end{bmatrix},$$

and get

$$\sum_{n=0}^{\infty} a_n |u_n\rangle = \sum_k E(\varepsilon_k) |\psi_k\rangle\langle\psi_k|g|\mathrm{vac}\rangle + E(0) \sum_i \left|\psi_i^{(0)}\right\rangle\left\langle\psi_i^{(0)}\right|g\left|\mathrm{vac}\right\rangle,$$

$$\sum_{n=0}^{\infty} a_n |V_n\rangle = \sum_k E(\varepsilon_k) |\Psi_k\rangle\langle\Psi_k|G|\mathrm{VAC}\rangle + E(0) \sum_j \left|\Psi_j^{(0)}\right\rangle\left\langle\Psi_j^{(0)}\right|G\left|\mathrm{VAC}\right\rangle,$$

$$\sum_{n=0}^{\infty} b_n |U_n\rangle = \sum_k I(\varepsilon_k) |\Psi_k\rangle\langle\psi_k|g|\mathrm{vac}\rangle,$$

$$\sum_{n=0}^{\infty} b_n |v_n\rangle = \sum_k I(\varepsilon_k) |\psi_k\rangle\langle\Psi_k|G|\mathrm{VAC}\rangle.$$

The vectors $|u_n\rangle, \ldots, |V_n\rangle$ can be computed recursively:

$$\begin{aligned} |u_0\rangle &= |\mathrm{vac}\rangle, \quad |U_0\rangle = \mathcal{Q}^\dagger |u_0\rangle, \\ |u_{n+1}\rangle &= 2\mathcal{Q}|U_n\rangle - |u_n\rangle, \\ |U_{n+1}\rangle &= 2\mathcal{Q}^\dagger |u_{n+1}\rangle - |U_n\rangle, \quad n \geq 0, \\ |V_0\rangle &= |\mathrm{VAC}\rangle, \quad |v_0\rangle = \mathcal{Q}|V_0\rangle, \\ |V_{n+1}\rangle &= 2\mathcal{Q}^\dagger |v_n\rangle - |V_n\rangle, \\ |v_{n+1}\rangle &= 2\mathcal{Q}|V_{n+1}\rangle - |v_n\rangle, \quad n \geq 0. \end{aligned}$$

4.1. *Distribution of Spectral Amplitudes*

In order to see how eigenconstituents of vectors $|\mathrm{vac}\rangle$ is target space and of $|\mathrm{VAC}\rangle$ in source space are distributed in the spectral range, we introduce the spectral density functions

$$\begin{aligned} \rho_{\mathrm{vac}}(\theta) &\stackrel{\text{def}}{=} \sum_{\theta_k > 0} \delta(\theta - \theta_k) |\langle\psi_k|g|\mathrm{vac}\rangle|^2 + \delta(\theta) \sum_i \left|\left\langle\psi_i^{(0)}\right|g\left|\mathrm{vac}\right\rangle\right|^2 \\ &= \sum_{n=0}^{\infty} a_n(\theta) \langle\mathrm{vac}|g|u_n\rangle \end{aligned} \tag{37}$$

and

$$\rho_{\mathrm{VAC}}(\theta) \stackrel{\mathrm{def}}{=} \sum_{\theta_k>0} \delta(\theta-\theta_k)|\langle\Psi_k|G|\mathrm{VAC}\rangle|^2 + \delta(\theta)\sum_j \left|\left\langle\Psi_j^{(0)}\right|G\left|\mathrm{VAC}\right\rangle\right|^2$$
$$= \sum_{n=0}^{\infty} a_n(\theta)\langle\mathrm{VAC}|G|V_n\rangle,$$

where the window $a_n(\theta)$ is given by (24) and $s_k = \sin(\theta_k/2)$. The procedure of their evaluation is evident from the above formulas.

In analogy with Section 3.3 distribution of singular values relevant to the target space is described by a function

$$\rho_{\mathcal{Q}}^{(T)}(\theta) = \delta(\theta)\,\mathrm{Dim}[\mathrm{Null}(\mathcal{Q}^\dagger)] + \sum_{\theta_k>0}[\delta(\theta-\theta_k)+\delta(\theta+\theta_k)]$$
$$= \mathrm{Mean}_{\mathrm{vac}}\{\rho_{\mathrm{vac}}(\theta)\}, \tag{38}$$

where $\mathrm{Dim}[\mathrm{Null}(\mathcal{Q}^\dagger)]$ is a dimension of the kernel of $\mathcal{Q}^\dagger$ and averaging is done over an ensemble of random vectors $|\mathrm{vac}\rangle = g^{-1/2}|\xi\rangle$ (see above).

5. SPECTRAL ANALYSIS OF THE LAPLACE TIDAL MODEL

To demonstrate the method in action, we shall consider the classical Laplace tidal model as an example. It takes into account only horizontal movements of a fluid on a planet and describes an ocean by linearized shallow water equations. Shallow water equations are equivalent to 2D barotropic hydrodynamics, where the internal energy of the fluid only depends on density. This ensures that we have a Newtonian mechanical system with nonpathological properties.

To specify the model, we need two scalar functions: the depth H of the ocean and the local Coriolis frequency Ω, which is just a projection of the planet's angular velocity on the local vertical axis. The dynamical variables are the vector field $\boldsymbol{v}$, which represents depth-averaged velocity of water, and a scalar field ζ, which represents departure of the sea surface from the geopotential surface.

The equations of free motion are the following:

$$\dot\zeta + \mathrm{div}(H\boldsymbol{v}) = 0, \tag{39}$$

$$\dot{\boldsymbol{v}} - 2\Omega(*\boldsymbol{v}) + g\nabla\zeta = 0. \tag{40}$$

Here g is acceleration due to gravity, $*$ denotes the counterclockwise (when looking from outer space) 90°-revolution of a tangent plane about the normal (vertical) axis and connects the directions of the velocity of a moving particle and the Coriolis force.

For convenience of consideration we shall combine the velocity and pressure fields in a unique field, φ, and rewrite (39)–(40) as $\dot\varphi = \mathcal{L}\varphi$. Particular details about the structure of the field φ and operator $\mathcal{L}$ may be found in Appendix B. The space of all possible configurations of φ shall be addressed as the phase space.

It may be shown that $\mathcal{L}$ is anti-self-adjoint with respect to the scalar product generated by the quadratic form of energy and, therefore, any configuration φ of the physical fields may be represented as a superposition of its eigenvectors.

For illustrative purposes we shall put the depth of the ocean and the local Coriolis frequency constant throughout the globe and assume it is a closed compact surface. The model describes steady gyres and rapid surface waves with phase velocity $c = \sqrt{gH}$. The spectrum of free oscillations is discrete and eigenmodes may be described in terms of eigenfunctions of the Laplace–Beltrami operator. Each eigenfunction of the Laplacian corresponding to an eigenvalue $\varepsilon > 0$ also corresponds to a steady solution of the tidal equations (to a geostrophic motion with zero frequency) and to two oscillatory surface gravity waves with frequency $\sqrt{4\Omega^2 + c^2\varepsilon}$. All these three modes exhibit the same shape of surface elevation which coincides with the matching eigenfunction of the Laplacian, but different character of fluid motion. If our 2D planet is topologically different from a sphere, there are also $2h$ inertial modes, where h is the genus (the number of "handles" glued to a sphere) of a geoid. All of them have the same frequency, 2Ω, null surface elevation, and are just uniform parallel flows which rotate under the action of the Coriolis force.

With such a full description in mind we composed a finite element numerical model on a torus-like geoid (see Appendices A and B) and checked its spectral properties against those of the actual continuous one. First, we generated an ensemble of three random vectors and used (27) for evaluation of density of states. Figure 1a presents a smoothed spectral density obtained via truncation of series (27), and Fig. 1b depicts its integral, the cumulative distribution

$$N(\omega) = \frac{\mathrm{Dim}_{\mathrm{null}}}{\mathrm{Dim}_{\mathrm{full}}} + \frac{2}{\mathrm{Dim}_{\mathrm{full}}} \int_0^{\omega} \sum_{0<\omega_k} \delta(\omega' - \omega_k)\, d\omega'.$$

Here ω_k stand for eigenfrequencies, $\mathrm{Dim}_{\mathrm{full}}$ and $\mathrm{Dim}_{\mathrm{null}}$ denote the full dimension of the phase space and of the null subspace of $\mathcal{L}$, respectively, and the factor 2 before the integral is necessary because there are two eigenvectors corresponding to each eigenfrequency $\omega_k > 0$. The value $N(\omega)$ is just the fraction of eigenmodes whose frequency do not exceed ω.

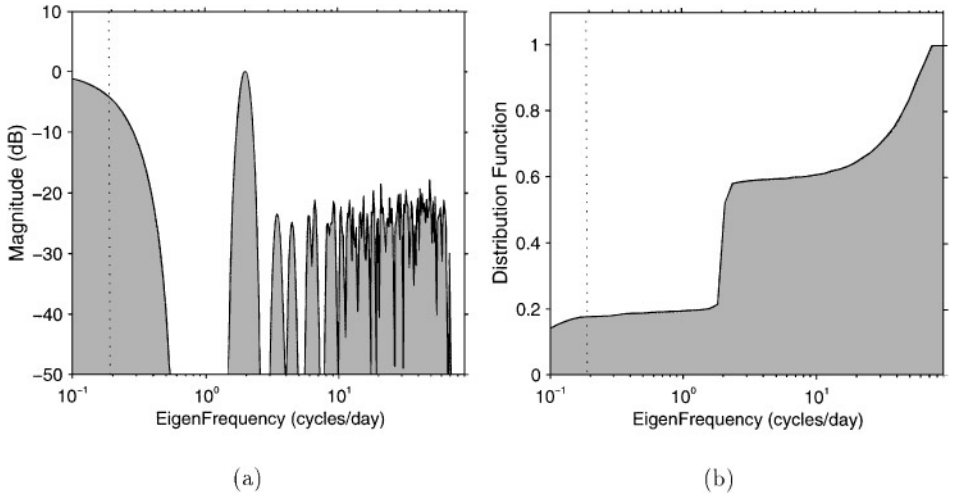

FIG. 1. Density (27) of eigenstates versus eigenvalues, (a), and cumulative distribution of eigenmodes in the spectral range of the numerical model, (b). The Chebyshev and Cezaro filters were used for smoothing δ-peaks in both graphs. The dotted line points at the frequency determined by the uncertainty principle (due to truncation of series (27)) and showing resolution in the frequency range.

The phase space of the actual finite element model had $\mathrm{Dim}_{\mathrm{full}} = 5120$ degrees of freedom, and each of them might be exited as an oscillation of a particular shape. From our consideration of the continuous model we could expect that the geostrophic sector would occupy about $1/3$ of the phase space and the gravity waves sector about $2/3$, with a negligible share of inertial sector. However, Fig. 1a shows a high peak at the inertial frequency, and from Fig. 1b we see that the inertial sector is as large as the gravity one. This numerically revealed discrepancy is due to the structure of our finite element model: analytical investigation shows that on a uniform grid with $M \times N$ nodes there exist $2MN$ holomorphic covector fields (only two of them must survive in the continuous limit), and each gives rise to an inertial oscillation.

Whereas the major part of the spectrum corresponding to gravity waves at given resolution looks as being continuous, near the low-frequency boundary it is obviously discrete. Zooming enables us to determine periods of the most slow eigenmodes in the gravity sector of the model: 400, 306, and 226 min.

Second, with the aid of the Fourier transform we were able to compose a synthetic wave pattern with known contributions from the geostrophic and gravity sectors: $\varphi = \varphi_{\mathrm{R}} + \varphi_{\mathrm{G}}$. Figure 2a shows the flow structure originating from superposition of two geostrophic modes and one gravity wave, and in Figs. 3a and 3b we can see the components φ_{R} and φ_{G} separately. This separation was achieved by applying a projecting operator on the invariant subspace of $\mathcal{L}$ forming the geostrophic sector to the field φ and, since this operator may be represented as a function of $\mathcal{L}$, its action was evaluated as described in Section 3.4: $\varphi_{\mathrm{R}} = F(\mathcal{L})_{\varphi}$ with

$$F(\omega) = \begin{cases} 1, & \text{if } |\omega| \le \omega_*, \\ 0, & \text{if } |\omega| > \omega_*. \end{cases} \tag{41}$$

Here $0 < \omega_* < 2\Omega$ is a frequency such that it separates the lower boundary, 2Ω, of the gravity sector from the geostrophic sector. The other constituent, φ_{G}, is equal to $\varphi - \varphi_{\mathrm{R}}$.

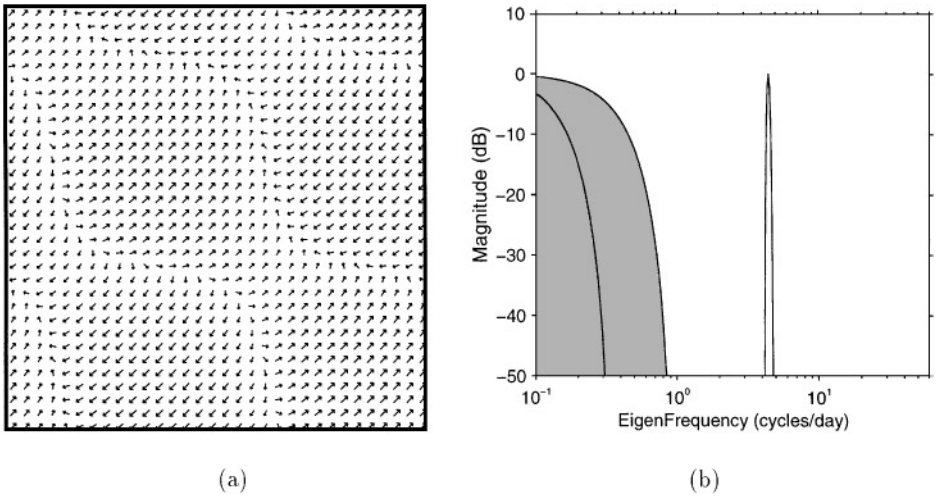

FIG. 2. The flow structure arising as a combination of two geostrophic modes and one gravity wave, (a), and the corresponding spectral function (26) (solid curve) together with the employed approximation to the projecting window (41) (boundary of the shaded area), (b).

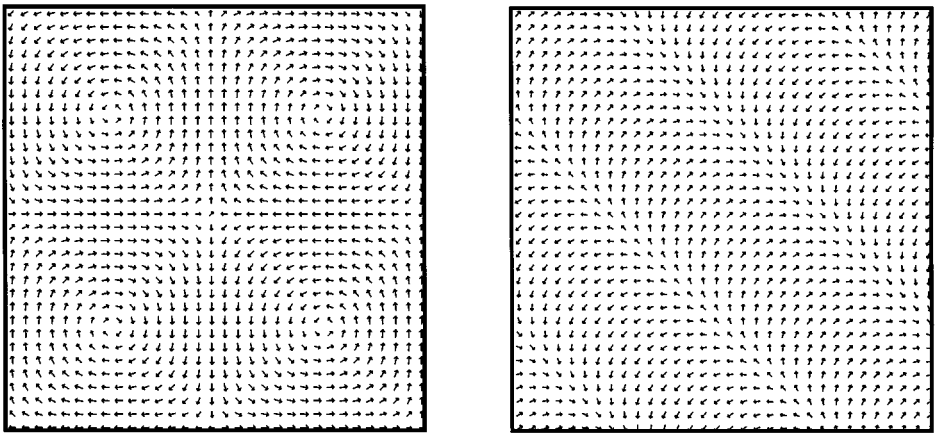

(a) (b)

FIG. 3. The flow structure of the geostrophic, (a), and gravity, (b), contributions to the flow shown in Fig. 2a.

Surely, instead of the exact value of $F(\mathcal{L})$, we computed an approximation $P(\mathcal{L})$ to it, with $P(\omega)$ being a polynomial. Its degree is a function of the required accuracy of approximation and of the ratio $\omega_{\max}/\omega_*$, where $\omega_{\max}$ is the maximum eigenfrequency of the numerical model. The shape of the employed polynomial is shown in Fig. 2b with the spectral function (26) corresponding to $|\mathrm{vac}\rangle = \varphi$ in the background. Note that in the logarithmic scale the width of the δ-peak corresponding to the geostrophic contribution looks much wider than that corresponding to the gravity wave. Needless to say that, since unwanted modes (gravity for Fig. 3a and geostrophic for Fig. 4a) were suppressed by a

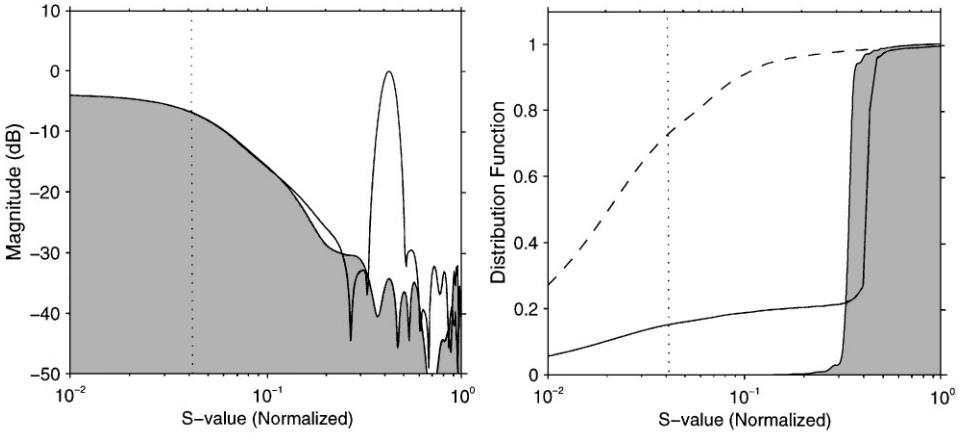

(a) (b)

FIG. 4. Spectral density (37) of noisy data (solid curve) and of noise only (boundary of the shaded area) as functions of singular values, (a), and corresponding cumulative distributions (44) (solid and dashed curves, respectively), together with the employed inverting window $I(s)$ (boundary of the shaded area shows the ratio $I(s)/s^{-1}$ of the regularized and exact windows) versus singular values, (b). The dotted line has the same meaning as in Fig. 1.

factor of $10^{5/2}$, one cannot visually distinguish these numerically obtained pictures from those similar but analytically constructed.

6. SOLUTION TO AN INVERSE PROBLEM BY SPECTRAL SYNTHESIS

Another interesting application is the problem of reconstructing large-scale oceanic circulation from the sea surface height (SSH) data. Collected by satellites, such data are of high accuracy at large scales and might be used for subsurface imaging of oceanic currents. Time averaging removes fast gravity waves from the SSH signal and we may assume that the resulting deviation of the sea surface from the geopotential surface in the framework of the Laplace model is only due to exited modes from the geostrophic sector. Thus, we are faced with a problem of spectral synthesis: find a state φ of the ocean, such that it is a superposition of slow eigenmodes of the hydrodynamic system and meets experimental data. This requirement of consistency with data shall be expressed in the classic way adopted in the geophysical community. Let $\mathcal{P}$ be the spectral projector on the slow subspace, let $\mathcal{O}$ be an orthogonal projector on the subspace with zero velocity of the fluid, and let $\mathcal{Q} \stackrel{\text{def}}{=} \mathcal{O}\mathcal{P}$ be the observation operator which maps the space of possible system configurations into the data space. Namely, it extracts the slow geostrophic component of φ and computes its contribution to the observed surface elevation ζ. The consistency means that in a sense equation $\mathcal{Q}\varphi = \zeta$ must hold.

In order to obtain a well-posed inverse problem, we have to equip the data and phase spaces with prior statistics which reflect our knowledge about the experimental tool and dynamical system. Normally in assimilation schemes it is assumed that these statistics are either uniform or Gaussian, with known mean and covariance. In our case we put prior statistics in both spaces to be Gaussian with zero mean. The covariance matrix in the phase space shall be determined by the quadratic form of energy (the sum of kinetic and potential energy of the fluid), and in data space it shall be supposed to coincide with the ordinary L_2-scalar product of functions defined on the globe. Note that, since the sum of signal and noise contributions to the observed variables is known (it is equal to data), we always get estimates of signal and noise in the data space simultaneously; given an estimate of a signal, we get an estimate of noise by simple subtraction, and vice versa.

Employing (30) we can state that the solution to our inverse problem may be obtained through singular value decomposition of the operator $\mathcal{Q}$:

$$\varphi = \sum_{s_k > 0} \frac{1}{s_k} (\psi_k, \zeta) \Psi_k. \tag{42}$$

Here $(\ldots, \ldots)$ is the scalar product in data space, $s_k > 0$ stand for nonzero singular values of $\mathcal{Q}$, Ψ_k and ψ_k are the corresponding normalized singular vectors in the phase and data spaces, respectively. They may be obtained as solutions to Eqs. (32)–(33). Operator $\mathcal{Q}^\dagger$ is the adjoint of $\mathcal{Q}$ with respect to Euclidean structures in the data and phase spaces which were specified before. Note that singular values and vectors not only do depend on the observation operator $\mathcal{Q}$, but on Euclidean structures as well, i.e., on our prior knowledge about stochastic properties of the noise which contaminates data and expected configuration of the hydrodynamic field φ.

In the case of our toy planet it is easy to find the singular value decomposition analytically. It appears that with the choice (41) for the projector $\mathcal{P} = \pi(\mathcal{L})$ one may take the set of

L_2-normalized Laplace's eigenfunctions for $\{\psi_k\}$, the set of corresponding geostrophic motions for $\{\Psi_k\}$ (normalized with respect to the quadratic form of energy), and the set $\{s_k = 2\Omega/\sqrt{4\Omega^2 + c^2\varepsilon_k}\}$ (with ε_k being the Laplacian eigenvalues) for the corresponding singular values. All gravity and inertial motions lie in the kernel of $\mathcal{Q}$ and were denoted as $\Psi_j^{(0)}$ in Section 4. We see that large-scale geostrophic motions corresponding to small eigenvalues ε_k are best observed. Note that in case of a torus eigenvalues of the Laplacian correspond to wavenumbers.

It is well known that one should not attempt to perform summation in (42) over all nonzero singular values, for this may lead to situations where a major part of the information is drawn from the noise. A good way to take control of things is to sum only over those singular values which are not very small in comparison with the largest one and which correspond to spectral amplitudes (ψ_k, ξ) of relatively large magnitude. Both cutoff levels are determined by signal/noise ratio. In other words, instead of the exact inverting window $1/s$ it is reasonable to use a regularized selective window, $I(s)$:

$$\varphi = \sum_{s_k > 0} I(s_k)(\psi_k, \zeta)\Psi_k. \tag{43}$$

In order to make a proper choice for the inverting window it is important to know how data are distributed in the spectral sense, i.e., whether large or small amplitudes (ψ_k, ζ) correspond to major singular values. Constituents corresponding to zero or small singular values cannot be represented by the observation operator, while those corresponding to large singular values are representable and may easily be reconstructed. Quantitatively this distribution is described by the spectral density (37). In practice, especially when the dimension of the data space exceeds several thousands, or when the same singular value corresponds to several singular vectors and the delta-peaks overlap, instead of (37) it is worthwhile to use the cumulative distribution function,

$$\mathcal{S}(s) \stackrel{\text{def}}{=} \sum_i \left|\left(\psi_i^{(0)}, \zeta\right)\right|^2 + \sum_{0<s_k<s} |(\psi_k, \zeta)|^2, \tag{44}$$

which is just the integral of (37). In order to see how noise contaminates data, we may generate it artificially and perform its spectral analysis with respect to the observation operator via formulas (37) and (44). Overlaying the plots of the experimentally collected data and of the artificially generated noise spectral densities, we may get an idea about the signal/noise ratio in different spectral bands and compose a proper inverting window $I(s)$.

For numerical demonstration we composed a large-scale current as a mixture of two geostrophic modes with the parameters as in the previous section and contaminated the resulting surface elevation (its maximum value was about 40 cm) with a random noise of 10 cm amplitude, forming a synthetic data which served as an input $|\text{vac}\rangle$ for processing according to Section 4. Distribution of spectral amplitudes, (37) and (44), are presented in Figs. 4a and 4b, together with similar distributions of an artificially generated noise (obtained by a different run of the random generator). The plots clearly show that we have a tool for selecting a signal from noisy data. Employing the inverting window shown in Fig. 4b, we were able to suppress 97% of the noise and to retain 80% of the signal power. The reconstructed velocity field agrees well with the original circulation pattern shown in Fig. 3a.

7. CONCLUSION

We have introduced a new approach for iterative solution to problems of spectral analysis/synthesis with respect to symmetric operators. Only little *a priori* spectral information is required, and it may be cheaply obtained numerically. Employing the methods of signal processing for the design of optimal windows allows us to determine the necessary number of iterations and the accuracy of approximation beforehand. In comparison with conventional matrix decomposition methods our finite-storage algorithm allows us to evaluate the action of operators represented by full matrices which cannot be either stored or even computed explicitly. Since we access the operator only via its action (see recursive formulas in Sections 3.1 and 3.4), its possible sparsity may be advantageously exploited. The major drawback of the method comes from its sequential nature which is not favorable for parallelization.

APPENDICES

A. *The Geoid*

By definition a geoid is a 2D closed surface equipped with Riemannian metric (say, inherited from the ambient 3D space). The corresponding measure of a 2D volume shall be denoted with $d\mu$. Counterclockwise 90°-revolution of the tangent plane about the normal (vertical) axis serves as a natural complex structure on a geoid and may be used for the selection of holomorphic coordinates [4].

For an invariant formulation of hydrodynamics it is convenient to use the calculus of external differential forms. In 2D the space of forms consists of three subspaces: $\mathcal{E}^{(0)}$, $\mathcal{E}^{(1)}$, and $\mathcal{E}^{(2)}$. They are formed by scalar functions, covector fields, and antisymmetric tensors of rank 2, respectively. The linear space of all such fields will be supplied with Hodge's scalar product,

$$(\varphi, \varphi') \stackrel{\text{def}}{=} \int (*\varphi) \wedge \varphi', \tag{A.1}$$

where φ and φ' are external forms, and $*$ stands for the unitary Hodge's operator acting as follows: if z is a local holomorphic coordinate and f is an arbitrary function, then

$$*f = f\, d\mu, \quad *f\, d\mu = f,$$
$$*f\, dz = if\, dz, \quad *f\, d\bar{z} = -if\, d\bar{z}.$$

All subspaces $\mathcal{E}^{(p)}$ are connected by invariant linear operators as shown in Fig. 5, where d_q and $*_q$ denote restrictions of external differentiation and Hodge's operator on $\mathcal{E}^{(q)}$, respectively. These relations appear important for the definition to finite-dimensional approximations to velocity and pressure spaces.

In 2D we only need to specify nonpathological $\mathcal{E}^{(0)}$, $\mathcal{E}^{(1)}$, $*_1$, d_1, and the measure $d\mu$. Then requirements of self-consistency uniquely determine $\mathcal{E}^{(2)}$ and d_2. Indeed, the structure of Hilbert space, introduced by (A.1), implies that $\mathcal{E}^{(2)}$ is isomorphic to $\mathcal{E}^{(0)}$, and it also determines the adjoint operator $d_1^\dagger$. In continuous theory $d_2^\dagger = *_1 d_1 *_2$ must be valid; thus, $d_2^\dagger$ and its adjoint, d_2, are also determined. All interesting operators may be represented in terms of them, say, divergence is $-d^\dagger$, and Laplacian is $-(d^\dagger d + d d^\dagger)$.

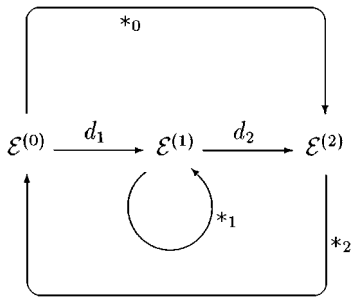

FIG. 5. Main invariant operators in the space of differential forms.

B. *2D Finite Element Hydrodynamics*

Instead of the vector field $\boldsymbol{v}$ it is convenient to use its rescaled dual, a covector field $\boldsymbol{w}$. In local coordinates x^1, x^2 we put $w_i \stackrel{\text{def}}{=} c g_{ik} v^k$, where $\boldsymbol{v} = v^i \partial/\partial x^i$, $\boldsymbol{w} = w_i\, dx^i$, and $g_{ik}\, dx^i \otimes dx^k$ stands for the metric tensor. Also, instead of ζ we shall use the scalar field $w \stackrel{\text{def}}{=} g\zeta$. In these variable equations of motion (39)–(40) take the form

$$\dot{w}\, d\mu - d(*c\boldsymbol{w}) = 0, \tag{B.1}$$

$$\dot{\boldsymbol{w}} - 2\Omega\,(*\boldsymbol{w}) + c\, dw = 0. \tag{B.2}$$

The velocity and pressure fields may be combined in a unique field $\varphi \stackrel{\text{def}}{=} w + \boldsymbol{w}$. This field takes values in the external algebra of cotangent bundle to the geoid. The linear space of all such fields will be equipped with Hodge's scalar product (A.1). An antisymmetric operator $\mathcal{L}$, defined by

$$\mathcal{L} : w + \boldsymbol{w} \mapsto 2\Omega\,(*\boldsymbol{w}) + d^\dagger(c\boldsymbol{w}) - c\, dw,$$

represents an antisymmetric bilinear form $\varphi \otimes \varphi' \mapsto (\varphi, \mathcal{L}\varphi')$, which is connected with Poisson brackets in the space of functionals of the field φ:

$$\{\mathcal{F}, \mathcal{G}\} \stackrel{\text{def}}{=} \left(\frac{\delta\mathcal{F}}{\delta\varphi}, \mathcal{L}\frac{\delta\mathcal{G}}{\delta\varphi}\right).$$

Here the variational derivative $\delta\mathcal{F}/\delta\varphi$ of a functional $\mathcal{F}$ is regarded as a tangent vector to the space of φ-fields, satisfying

$$\delta\mathcal{F} = \left(\frac{\delta\mathcal{F}}{\delta\varphi}, \delta\varphi\right)$$

for any infinitesimal field $\delta\varphi$. With these definitions equations (B.1)–(B.2) can be written in Hamiltonian form, i.e.,

$$\dot{\varphi} = \{\varphi, \mathcal{G}\}, \tag{B.3}$$

where Hamiltonian $\mathcal{G}$ coincides with the sum of the kinetic and potential energies of the fluid. Its value is just the squared Hodge's norm of the field φ:

$$\mathcal{G} = \frac{1}{2}\int (w^2 + |\boldsymbol{w}|^2)\, d\mu = \frac{1}{2}(\varphi, \varphi).$$

Equations (B.3) are nothing but $\dot{\varphi} = \mathcal{L}\varphi$ rewritten in variational form. Note, that our system is neutrally stable, because the spectrum of the dynamical operator $\mathcal{L}$ is purely imaginary and there are no nontrivial Jordan blocks.

For a formulation of discrete hydrodynamics we need finite-dimensional interpolation spaces for representation of the pressure and velocity. To obtain them, we approximated the surface of a torus-like geoid by plane 2D triangular elements, and assumed its geometry to be plain Euclidean. Scalar fields were represented by piecewise affine continuous functions; any function of this kind is uniquely determined by its values at the nodes of the mesh. Covector fields were considered to be piecewise constant, attaining constant values on particular elements. Therefore, the metric tensor also was constant throughout each separate element.

We defined that a covector field is closed if its restrictions to any segment from different adjacent elements equal each other. In this case an integral of a closed covector field along a homologically trivial cycle is equal to zero. We also prescribe that external differentiation maps the space of scalar fields into covectors in a natural manner, resulting in piecewise constant covectors. Simple considerations show that the dimension of the factor space of closed covector fields modulo exact ones is equal to the first Betti number of the geoid, as is necessary.

In the framework of the outlined variational formulation we do not need to specify explicitly how finite element cells are related with each other by the Levi–Civita connection and we may restrict dynamical equations to any subspace of the full phase space.

In order to remain in the framework of geophysics we made the dimensions of the torus equal to the Earth's radius, the ocean depth to 5 km, and the Coriolis frequency correspond to one revolution in a day.

C. *Odd Windows via Fast Fourier Transform*

To compute the coefficients $\{b_n\}$ for an odd window

$$I(\varepsilon) = \sum_{n=0}^{\infty} b_n T_{2n+1}(\varepsilon), \quad |\varepsilon| < 1, \tag{C.1}$$

we substitute $\sin(\theta/2)$ for ε in (C.1) and get

$$I\left(\sin\frac{\theta}{2}\right) = \sum_{n=0}^{\infty}(-1)^n b_n \sin\left(n+\frac{1}{2}\right)\theta, \quad |\theta| < \pi.$$

If only a finite number of coefficients are nonzero, we can solve this equation by the fast Fourier transform. Specifically, given an odd function $\gamma(\theta)$,

$$\gamma(\theta) = \sum_{n=0}^{N-1} \beta_n \sin\left[\left(n+\frac{1}{2}\right)\theta\right], \tag{C.2}$$

we only need to evaluate it at the points

$$\theta_m = \frac{\pi}{N}\left(m+\frac{1}{2}\right), \quad m = 0, \ldots, N-1,$$

and use the following reconstruction formula:

$$\beta_n = \frac{2}{N}\sum_{m=0}^{N-1} \sin\left[\frac{\pi}{N}\left(n+\frac{1}{2}\right)\left(m+\frac{1}{2}\right)\right]\gamma(\theta_m). \tag{C.3}$$

Thus, $b_n = (-1)^n\beta_n$, where β_n are given by (C.3) and

$$\gamma(\theta) = I\left(\sin\frac{\theta}{2}\right).$$

D. *Even Windows via Fast Fourier Transform*

Evaluation procedure for even windows is similar to the above one. Substituting $\sin(\theta/2)$ for ε in

$$E(\varepsilon) = \sum_{n=0}^{\infty} a_n \mathrm{T}_{2n}(\varepsilon), \quad |\varepsilon| < 1, \tag{D.1}$$

we obtain

$$E\left(\sin\frac{\theta}{2}\right) = \sum_{n=0}^{\infty}(-1)^n a_n \cos(n\theta), \quad |\theta| < \pi.$$

Given an even trigonometric polynomial $\gamma(\theta)$,

$$\gamma(\theta) = \sum_{n=0}^{N-1} \alpha_n \cos(n\theta),$$

we have to evaluate it at the points $\theta_m = \pi m/N$ and use

$$\begin{aligned}
\alpha_0 &= \frac{1}{N}\sum_{m=1}^{N-1}\gamma(\theta_m) + \frac{1}{2N}[\gamma(0)+\gamma_*],\\
\alpha_n &= \frac{2}{N}\sum_{m=1}^{N-1}\cos\left(\frac{\pi nm}{N}\right)\gamma(\theta_m) + \frac{1}{N}[\gamma(0)+(-1)^n\gamma_*],\\
\gamma_* &\stackrel{\text{def}}{=} (-1)^{N-1}\left[\gamma(0) + 2\sum_{m=1}^{N-1}(-1)^m\gamma(\theta_m)\right].
\end{aligned}$$

Thus, we put $a_n = (-1)^n\alpha_n$, where the coefficients α_n must be computed according to the above formulas, and

$$\gamma(\theta) = E\left(\sin\frac{\theta}{2}\right).$$

REFERENCES

1. H. Bateman, *et al*., *Higher Transcendental Functions, Vol. 2* (McGraw–Hill, New York, 1953).
2. R. W. Hamming, *Digital Filters* (Prentice–Hall, Englewood Cliffs, NJ, 1977).
3. T. W. Parks and C. S. Burrus, *Digital Filter Design* (Wiley, New York, 1987), p. 83.
4. R. Wells, *Differential Calculus on Complex Manifolds* (Wiley, New York, 1976), p. 779.